NeuroImage: Clinical 35 (2022) 103053

Contents lists available at ScienceDirect

NeuroImage: Clinical

journal homepage: www.elsevier.com/locate/ynicl

Brain temperature as an indicator of neuroinflammation induced by typhoid vaccine: Assessment using whole-brain magnetic resonance spectroscopy in a randomised crossover study

Julia R. Plank [a,*], Catherine Morgan [b,c], Frederick Sundram [d], Lindsay D. Plank [e], Nicholas Hoeh [d], Sinyeob Ahn [f], Suresh Muthukumaraswamy [a], Joanne C. Lin [a]

[a] School of Pharmacy, Faculty of Medical and Health Sciences, University of Auckland, 85 Park Road, Grafton, Auckland 1023, New Zealand
[b] Centre for Advanced MRI, Auckland UniServices Limited, 85 Park Road, Grafton, Auckland 1023, New Zealand
[c] School of Psychology and Centre for Brain Research, University of Auckland, 23 Symonds Street, Auckland 1010, New Zealand
[d] Department of Psychological Medicine, School of Medicine, Faculty of Medical and Health Sciences, University of Auckland, 22-30 Park Avenue, Grafton, Auckland 1023, New Zealand
[e] Department of Surgery, School of Medicine, Faculty of Medical and Health Sciences, University of Auckland, 22-30 Park Avenue, Grafton, Auckland 1023, New Zealand
[f] Siemens Medical Solutions, 40 Liberty Boulevard, Malvern, PA 19355, United States

ARTICLE INFO

Keywords:
Neuroinflammation
Brain temperature
Magnetic resonance spectroscopy
Echo-planar spectroscopic imaging
Metabolites
Mood
Typhoid vaccine

ABSTRACT

Prior studies indicate a pathogenic role of neuroinflammation in psychiatric disorders; however, there are no accepted methods that can reliably measure low-level neuroinflammation non-invasively in these individuals. Magnetic resonance spectroscopic imaging (MRSI) is a versatile, non-invasive neuroimaging technique that demonstrates sensitivity to brain inflammation. MRSI in conjunction with echo-planar spectroscopic imaging (EPSI) measures brain metabolites to derive whole-brain and regional brain temperatures, which may increase in neuroinflammation. The validity of MRSI/EPSI for measurement of low level neuroinflammation was tested using a safe experimental model of human brain inflammation – intramuscular administration of typhoid vaccine. Twenty healthy volunteers participated in a double-blind, placebo-controlled crossover study including MRSI/EPSI scans before and 3 h after vaccine/placebo administration. Body temperature and mood, assessed using the Profile of Mood States, were measured every hour up to four hours post-treatment administration. A mixed model analysis of variance was used to test for treatment effects. A significant proportion of brain regions (44/47) increased in temperature post-vaccine compared to post-placebo ($p < 0.0001$). For temperature change in the brain as a whole, there was no significant treatment effect. Significant associations were seen between mood scores assessed at 4 h and whole brain and regional temperatures post-treatment. Findings indicate that regional brain temperature may be a more sensitive measure of low-level neuroinflammation than whole-brain temperature. Future work where these measurement techniques are applied to populations with psychiatric disorders would be of clinical interest.

1. Introduction

Neuroinflammation, an inflammatory response located within the central nervous system, is observed in a variety of psychiatric and neurodegenerative conditions (Najjar et al., 2013; Schain and Kreisl, 2017). Understanding of neuroinflammation is currently limited, however, by the lack of non-invasive techniques. Brain temperature, measured using magnetic resonance spectroscopic imaging (MRSI), may be a useful measure of neuroinflammation (Babourina-Brooks et al., 2014; Karaszewski et al., 2009, 2013; Mueller et al., 2020a). Brain temperature is expected to increase in cases of neuroinflammation as microglial activation increases metabolic demands, leading to production of excess heat (Omori et al., 1997).

Increased brain temperature has been observed in previous studies of conditions associated with neuroinflammation such as ischaemic stroke (Karaszewski et al., 2009; Whiteley et al., 2012), brain tumours

* Corresponding author.
E-mail address: j.plank@auckland.ac.nz (J.R. Plank).

https://doi.org/10.1016/j.nicl.2022.103053
Received 24 March 2022; Received in revised form 16 May 2022; Accepted 17 May 2022
Available online 19 May 2022

(Babourina-Brooks et al., 2014), and myalgic encephalomyelitis/chronic fatigue syndrome (Mueller et al., 2020a). Very few studies have measured brain temperature in psychiatric disorders; however, elevated brain temperature in patients with schizophrenia has been observed using diffusion weighted imaging (DWI) based thermometry (Ota et al., 2014). DWI thermometry utilises the temperature dependence of the diffusion coefficient of cerebrospinal fluid (CSF) to estimate brain temperature. However, pulsatile movement, aging effects, and composition of substrates within the CSF may affect the accuracy of temperature results, and DWI thermometry does not provide regional information (Sumida et al., 2016).

MRSI is a non-invasive imaging technique that uses the signal from hydrogen protons (^{1}H) to detect and quantify chemical shifts of endogenous substances in the brain (Cady et al., 1995). MRSI is a valuable tool for measuring the temperature distribution across the brain as ^{1}H exhibits a chemical shift dependent on temperature whilst remaining stable with respect to other factors such as pH, enabling ^{1}H to act as an internal temperature probe (Cady et al., 1995; Ackerman et al., 1969). There is an almost linear dependence of the water ^{1}H resonance frequency on temperature between 0 °C and 40 °C, such that the resonance frequency shifts closer to a temperature independent metabolite by approximately 0.01 ppm/°C (Cady et al., 1995; Hindman, 1966). Use of a reference peak, such as total creatine (CR), enables a single-shot method where temperature is calculated as a function of the chemical shift of water relative to CR (Maudsley et al., 2017). Creatine remains stable against various factors such as pH and also shows reduced sensitivity to magnetic susceptibility changes at the cellular level (Ackerman et al., 1969; Kanai et al., 2001; Govindaraju et al., 2000).

In addition to temperature measurements, MRSI is useful for detecting inflammation-related alterations in the concentrations of metabolites such as choline-containing compounds (CHO), N-acetylaspartate (NAA), and myo-inositol (MI). Alterations in the metabolite concentrations have been observed in inflammatory disorders such as multiple sclerosis (Kirov et al., 2009), and in animal studies following administration of an acute inflammatory stimulus (Moshkin et al., 2014). CHO is involved in cellular turnover and membrane metabolism; increased CHO is observed in neuroinflammatory conditions and believed to represent membrane degradation or oedema (Chang et al., 2013; Michaelis et al., 1993). In contrast, decreased NAA is a marker of demyelination or axonal damage (Clark, 1998). MI is found primarily in astrocytes and is therefore regarded as a marker of glial content (Brand et al., 1993); higher concentrations of MI are observed in inflammatory conditions (Kirov et al., 2009; Chang et al., 2013).

Prior MRSI studies of neuroinflammation are limited by the use of single voxel spectroscopy, capturing only selected regions of the brain. MRSI in conjunction with 3D echo-planar spectroscopic imaging (EPSI) enables the capture of multi-voxel spectra, providing regional temperature information from the whole brain in clinically tolerable scan times (Sharma et al., 2020). Whole-brain measurements of brain temperature can then be computed by averaging spectra across all regions. Moreover, an *a priori* hypothesis is not required regarding the specific location of increased inflammation because temperature across the whole brain is investigated rather than only one or two regions. EPSI simultaneously acquires metabolite spectra and their spatial location in the brain, enabling shorter scan times than alternative multi-voxel techniques (Ebel and Maudsley, 2003).

In the present study, we aimed to investigate the feasibility of MRSI/EPSI for measurement of low level neuroinflammation, with potential applications for psychiatric disorders. Psychiatric disorders such as major depressive disorder (MDD) demonstrate low-level neuroinflammation, in contrast to medical conditions such as traumatic brain injury, stroke, meningitis, and multiple sclerosis which incur high levels of neuroinflammation as indicated by elevated concentrations of pro-inflammatory cytokines (Goldsmith et al., 2016; Osimo et al., 2018). The typhoid vaccine, containing 0.025 mg of purified Vi capsular polysaccharide of *Salmonella typhi,* safely induces a low level of neuroinflammation in healthy subjects 3–4 h after administration (Strike et al., 2004; Wright et al., 2005). Peripheral inflammatory markers suggest the level of inflammation induced by the typhoid vaccine is similar to that observed in MDD (Harrison et al., 2015).

We hypothesised that following the typhoid vaccine, but not placebo, participants would demonstrate elevated brain temperature across the whole brain and in regions associated with inflammation. We also expected to see metabolite alterations in regions of the brain consistent with the occurrence of an inflammatory response. Mood was expected to decline following administration of the vaccine, in agreement with prior studies on typhoid vaccine (Strike et al., 2004; Wright et al., 2005).

2. Materials and methods

2.1. Participants

Healthy volunteers were recruited through online advertisements, social media, and word of mouth. Volunteers between the ages of 18 to 55 were eligible to participate, unless they met any of the following exclusion criteria: i) presence of physical or psychiatric illness; ii) current use of anti-inflammatory medication; iii) recreational drug use within the previous six months; iv) smoking; v) hypersensitivity or reaction to typhoid vaccine; vi) receipt of a typhoid vaccine within the past three years, or any vaccine within one month; vii) elevated body temperature (>38 °C) or any peripheral indication of infection or illness; and viii) contraindications for MRI scanning. Older adults were excluded as they appear to respond to immune stimulation with an exaggerated response compared to younger individuals (Godbout et al., 2005; Chen et al., 2008). The first 20 eligible participants were invited to take part in the study. Ethical approval for the study was granted by the Northern Health and Disability Ethics Committee (19/NTB/8) and the trial was registered at ANZCTR (ACTRN12619000738123).

2.2. Study design

Participants gave written informed consent at an initial screening visit for eligibility. Following the screening, participants attended two study visits each in a randomised, double-blinded, placebo-controlled, crossover trial. Fig. 1 indicates the flow of participants through the trial and study visit protocol. A randomization sequence was generated by computer and an independent party allocated participants to one of two experimental groups (vaccine first then placebo, or placebo first then vaccine). Participants and investigators were blinded to treatment allocation. Each participant received the vaccine or placebo on a separate study visit. Each study visit was at least 7 days apart to allow for a sufficient wash-out period. The dose of typhoid vaccine was 0.5 mL of solution containing 0.025 mg of purified Vi capsular polysaccharide of *Salmonella typhi* (Ty 2 strain). The placebo dose was 0.5 mL of 0.9% saline solution. Both treatments were administered as an intramuscular injection in the deltoid of the arm.

2.3. Mood questionnaire

The Profile of Mood States (POMS) (McNair et al., 1971) was administered at baseline prior to treatment administration and at 1, 2, 3, and 4 h following treatment administration. POMS was used to assess any mood alterations associated with neuroinflammation. POMS comprises 65 adjectives and requires participants to rate their mood at the moment of assessment on a five-point scale from 0 (not at all) to 4 (extremely). Mood scores were calculated according to the POMS manual (McNair et al., 1971), culminating in 7 subscales of tension, depression, fatigue, anger, confusion, and vigour. Total mood disturbance was calculated by summing the negative mood subscales (tension, depression, fatigue, anger, confusion) and then subtracting the positive mood subscale (vigour). Overall mood was calculated in the same way but excluding the anger subscale (McNair et al., 1971; Wright et al.,

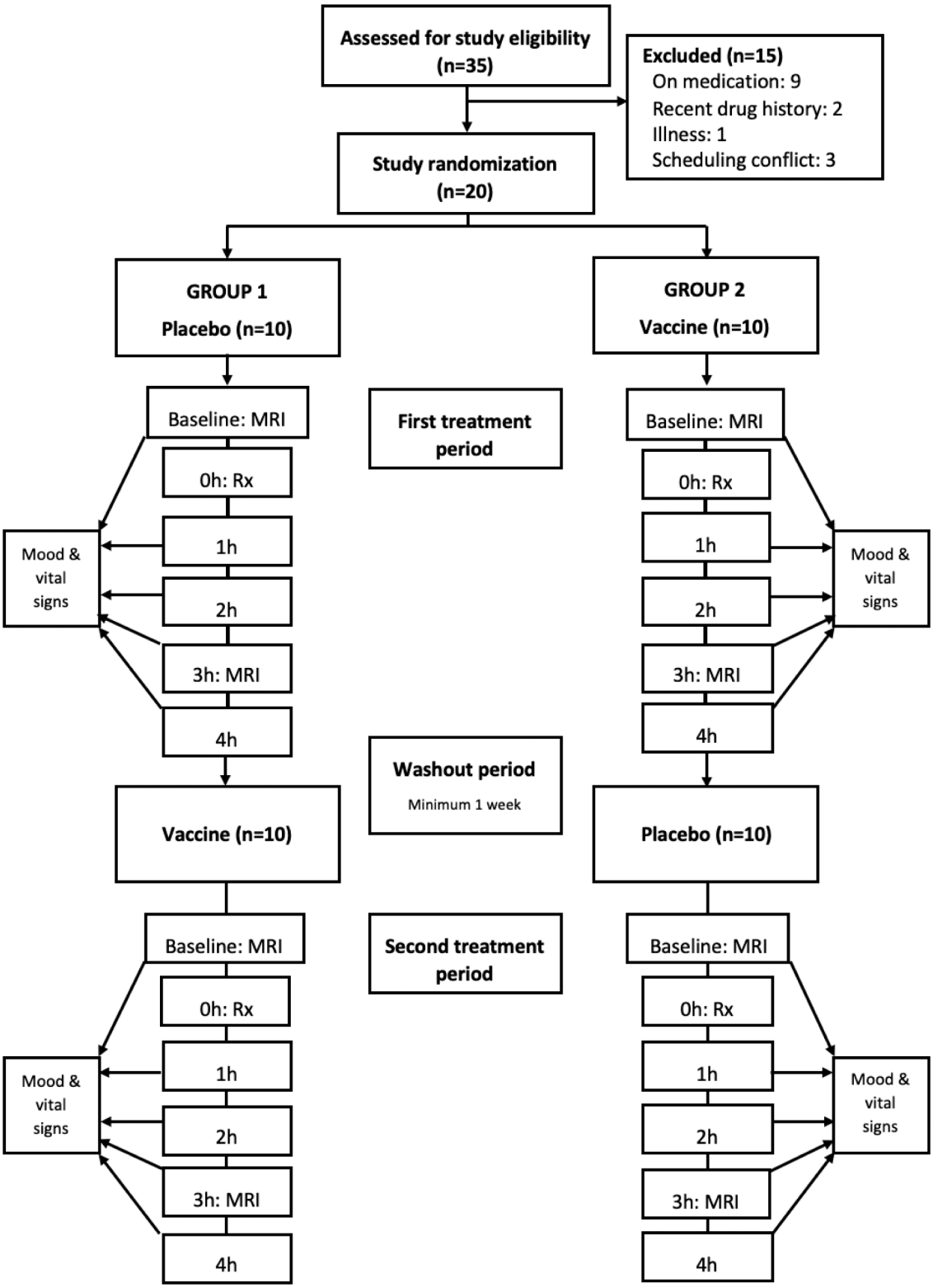

Fig. 1. Flow of participants through the study. *Note:* Rx = treatment (placebo/vaccine).

2005).

2.4. Vital signs

Heart rate, blood pressure, and body temperature were measured at baseline and at hourly intervals until 4 h post-treatment administration. Heart rate and blood pressure were measured using an electronic sphygmomanometer. Body temperature was measured in the right ear (Welch Allyn Braun Pro 6000 ThermoScan).

2.5. Image acquisition

Imaging data were collected using a MAGNETOM Skyra 3 T MRI scanner (Siemens Healthcare, Erlangen, Germany) with a 32-channel

head coil at baseline and at 3–4 h post-treatment. A T1-weighted image was acquired for segmentation and anatomical reference using a magnetization prepared rapid gradient echo (MPRAGE) sequence: repetition time (TR) = 2000 ms; echo time (TE) = 2.85 ms; inversion time (TI) = 880 ms; flip angle = 8°; 208 slices; slice thickness = 1.00 mm; field of view (FOV) = 256 × 256 mm; matrix = 256 × 256; voxel size = 1.0 × 1.0 × 1.0 mm; acquisition time (TA) = 4 min 56 s.

Whole-brain MRSI data were acquired using a 3D EPSI sequence: TR for metabolite data (TR1) = 1551 ms; TR for interleaved water reference data (TR2) = 511 ms; TE = 17.6 ms; lipid inversion nulling with TI = 198 ms; spin-echo excitation with selection of 140 mm axial slab covering the cerebrum; flip angle = 71°; FOV = 280 × 280 × 180 mm; matrix = 50 × 50 × 18; generalised autocalibrating parallel acquisitions factor (GRAPPA) factor = 1.3; voxel size = 5.6 × 5.6 × 10 mm; TA = 15 min 17 s. Interpolation was performed in the slice direction, yielding 32 slices of 5 mm thickness. The imaging FOV was acquired in a foot to head orientation and positioned to cover the whole brain. The metabolite and water reference signal datasets were obtained using the appropriate TR: the metabolite data were obtained using TR1 and the water reference data were obtained using TR2. An interleaved acquisition without water suppression was used to acquire the water reference signal (TE = 3.8 ms). The sequence included 1000 readout periods, each comprising 100 sample points (2x oversampling), and a spectral bandwidth of 9.8 ppm. Following reconstruction to correct for oversampling and the combination of odd and even echoes, the spectral bandwidth was reduced by half.

Prior to data acquisition, a 3D automatic shim was performed followed by an interactive shim where required to achieve an ideal full width at half maximum ≤ 30 Hz. A regional saturation band was also placed over the eyes to suppress signal from the eyes and sinuses, and off-resonance frequency correction was performed to correct for frequency drift.

2.6. Image processing

The Metabolite Imaging and Data Analysis System (MIDAS) software package (http://mrir.med.miami.edu) was used to process the MRSI data through a fully automated processing pipeline (Maudsley et al., 2009) including image reconstruction, correction for spatially-dependent B0 shifts, spatial registration to Montreal Neurological Institute space at 2 mm isotropic voxel resolution, interpolation to 64 × 64 × 32 points, and smoothing with a Gaussian kernel (5 mm in plane; 7 mm through plane). The effective voxel volume after spatial smoothing was 1.5 mL. FSL/FAST was used to segment the T1-weighted MRI images into white matter, grey matter, and CSF (Zhang et al., 2001). Resultant tissue maps were then registered to high-resolution structural images. The FITT2 module within MIDAS was used to carry out automated spectral fitting using Gaussian line shapes for all resonances, followed by normalization to institutional units using water as a reference. The water reference was acquired using a non-water-suppressed acquisition interleaved with the metabolite measurement. Whole brain temperature was determined using a voxel-wise approach, where the difference in chemical shift between the CR and water resonances were calculated according to the equation $T = -102.6 \times \Delta_{water-CR} + 206.1$ (Maudsley et al., 2017). The whole brain MRSI temperature maps were then spatially registered to MNI space for delineation of 47 regions of interest (ROIs) using a modified version of the Automated Anatomical Labeling (AAL) atlas (Tzourio-Mazoyer et al., 2002). The ROI-based approach was chosen due to the improved signal-to-noise ratio and reduced number of statistical tests (and false positives) required in comparison to a voxel-wise approach.

2.7. Data analysis

The Project Review and Analysis (PRANA) module and Map Integrated Spectrum (MINT) modules within MIDAS were used to analyse the MRSI data before statistical testing. An inverse spatial transformation algorithm within PRANA was used to convert the AAL-delineated regions into subject space. Spectral averaging was then completed in MINT in order to obtain average values of each metabolite (CR, CHO, MI, NAA) concentration, metabolite ratios, and brain temperature within each ROI. Voxels were excluded from spectral averaging based on the following quality criteria: i) fitted metabolite linewidth > 13 Hz; ii) having an outlying value >2.5 times the standard deviation of all valid voxels over the image; iii) a Cramér-Rao Lower Bound for fitting of CR of >20%; and iv) >30% CSF contribution to the voxel volume. Data quality was assessed post-processing based on the number (%) of accepted voxels. Representative spectra from a single voxel in a single subject are shown in Fig. 2.

To enable comparison with other studies, metabolites were expressed as ratios to CR. Data are available at Mendeley Data; https://doi.org/10.17632/tk2bthtvky.1.

2.8. Statistical analysis

Analysis was performed using a linear mixed model including group, period, brain region, and treatment as fixed factors, and patient (nested in group) as a random factor (Senn, 2002). Follow-up analysis excluded the fixed factor of brain region to test for treatment effects on each individual ROI. Later analysis included hemisphere as a fixed factor to test for hemispheric differences between regions. All mixed models were adjusted for baseline. The two-stage step-up method of Benjamini and Yekutieli (2001) was used to control the False Discovery Rate (FDR = 0.05) and correct *p*-values for multiple tests. Values of the dependent variable were visually examined for approximate normality and homoscedasticity. Z tests for comparisons of proportions were performed. Whole-brain temperature, regional brain temperatures, and regional metabolite ratios were tested for associations with body temperature and mood scores using Spearman's correlation coefficient (r_s). Results were considered statistically significant if $p < 0.05$. Analyses were performed using SAS 9.4 (SAS Institute, Cary NC). Data are presented as means ± standard error (SEM) unless otherwise specified.

3. Results

3.1. Participants

Two participants (Group 1) were excluded from analysis of the second period data due to pregnancy during washout period (n = 1) and consumption of anti-inflammatory medications (n = 1). A further participant (Group 1) was excluded from analysis of second period MRI data due to movement during acquisition. Participant characteristics at randomisation are detailed in Table 1.

3.2. Main results

Data from three MRI scans were excluded from statistical analysis due to poor data quality, indicated by < 30% of voxels accepted across the whole brain. The excluded MRI scans were all from period one: a baseline scan and post-treatment scan from Group 2, and a post-treatment scan from Group 1. Supplementary Figs. 1 and 2 show evidence of data quality. The average numbers and percentages of voxels accepted for analysis, alongside the average whole brain temperatures, are shown in Supplementary Table 1. There were no systematic differences in data quality observed between vaccine and placebo. There was no significant effect of treatment on whole brain temperature ($p = 0.18$). Initial mixed model analysis indicated a significant effect of treatment ($p < 0.0001$), brain region ($p < 0.0001$), and baseline brain temperature ($p < 0.0001$) on post-treatment brain temperature.

A significant proportion of brain regions (44/47) were at a higher temperature post-vaccine compared to post-placebo ($p < 0.0001$) as shown in Fig. 3. Mixed models for the 47 regional brain temperatures

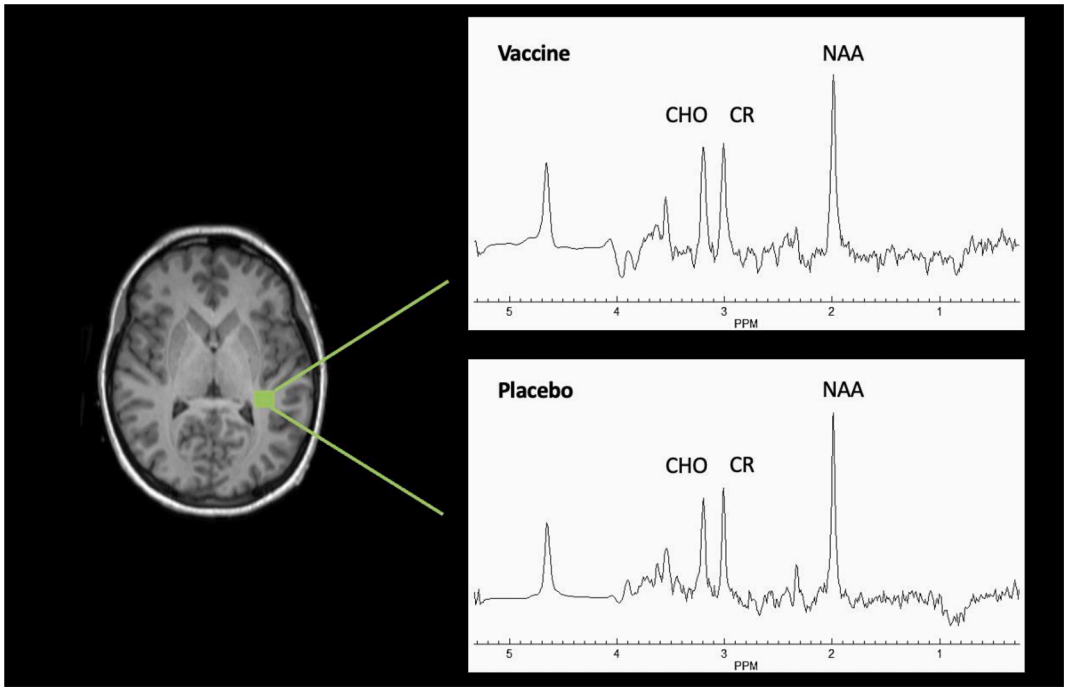

Fig. 2. Representative spectra from single voxel in a single subject post-vaccine and post-placebo administration. *Note:* Post-placebo ratios for NAA/CR and CHO/CR are 1.418 and 0.266 respectively; post-vaccine ratios for NAA/CR and CHO/CR are 1.337 and 0.297 respectively.

Table 1
Participant demographics and clinical characteristics at randomisation.

	All participants (n = 20)
Age	34 (18–44)
Sex (M/F)	10/10
Ethnicity	
European	8
Asian	8
Latin American	3
Middle Eastern	1
Weight (kg)	68.80 ± 14.08
Body temperature (^{O}C)	36.20 ± 0.35
Heart rate (bpm)	62.38 ± 9.35
Systolic blood pressure (mmHg)	116.1 ± 13.3
Diastolic blood pressure (mmHg)	72.53 ± 7.65

Data are presented as median (range), number of participants, or mean ± standard deviation.

found a significant effect of treatment on the right anterior cingulum ($p = 0.03$), and left occipital lobe ($p < 0.01$). Right anterior cingulum temperature was higher post-vaccine (36.86 ± 0.14) than post placebo (36.41 ± 0.12), a difference of 0.46 (95% CI: 0.05, 0.86)°C. Left occipital lobe temperature was also higher post-vaccine (37.03 ± 0.12) than post-placebo (36.79 ± 0.11), a difference of 0.24 (95% CI: 0.08, 0.40)°C. The mixed models did not reveal any further regions of significance. The effects of treatment in the two brain regions did not remain significant following corrections for multiple tests. The average temperature in each brain region post-vaccine and post-placebo are provided in Supplementary Table 3.

There was a significant effect of hemisphere on temperature in the precentral region ($p < 0.0001$), frontal lobe ($p < 0.0001$), calcarine ($p < 0.01$), postcentral region ($p < 0.0001$), putamen ($p = 0.01$) and caudate ($p = 0.03$). The confidence intervals are provided in Supplementary Table 2. Temperature was higher in the left hemisphere in all five regions. The effect of hemisphere remained significant following corrections for multiple tests in the precentral region ($p < 0.001$), frontal lobe ($p < 0.001$), calcarine ($p = 0.01$) and postcentral region ($p < 0.001$). On average, post-vaccine temperature was slightly higher in the left hemisphere (37.26 ± 0.08) than the right (37.13 ± 0.09).

3.3. Secondary results

3.3.1. Metabolites

Significant effects of treatment on the metabolite ratios are shown in Table 2. The effects of treatment did not remain significant following corrections for multiple tests. There were no significant treatment effects observed for metabolite ratios LAC/CR or NAA/CR in the 47 AAL atlas brain regions.

3.3.2. Body temperature

There were no significant correlations between whole brain temperature and body temperature post-vaccine. There were, however, several significant correlations identified between body temperature and whole brain temperature pre-vaccine, pre-placebo, and post-placebo as shown in Table 3 and in Supplementary Table 5. Mixed model analysis did not find any significant effect of treatment on body temperature. Average body temperatures post-vaccine and post-placebo are shown in Supplementary Table 4.

3.3.3. Mood

There was no significant effect of treatment on any of the seven mood subscales. Average mood scores post-vaccine and post-placebo are shown in Supplementary Table 6. The overall mood trajectories following placebo and vaccine are shown in Fig. 3. Significant correlations were found between post-vaccine whole brain temperature and total mood disturbance ($r_s = 0.492$, $p = 0.038$), tension ($r_s = 0.629$, $p = 0.005$), and confusion ($r_s = 0.491$, $p = 0.0038$) measured at 4 h, as shown in Supplementary Table 7. There were 80 (out of a possible 329) significant correlations between mood subscales and regional brain temperatures at 3 h post-vaccine and 37 at 4 h post-vaccine; a selection of these are shown in Supplementary Fig. 3. There were seven (out of 329) significant correlations between mood subscales and regional brain temperatures at 3 h post-placebo, and eight at 4 h post-placebo. All correlations between regional brain temperatures and mood subscales are shown in Supplementary Tables 8 and 9.

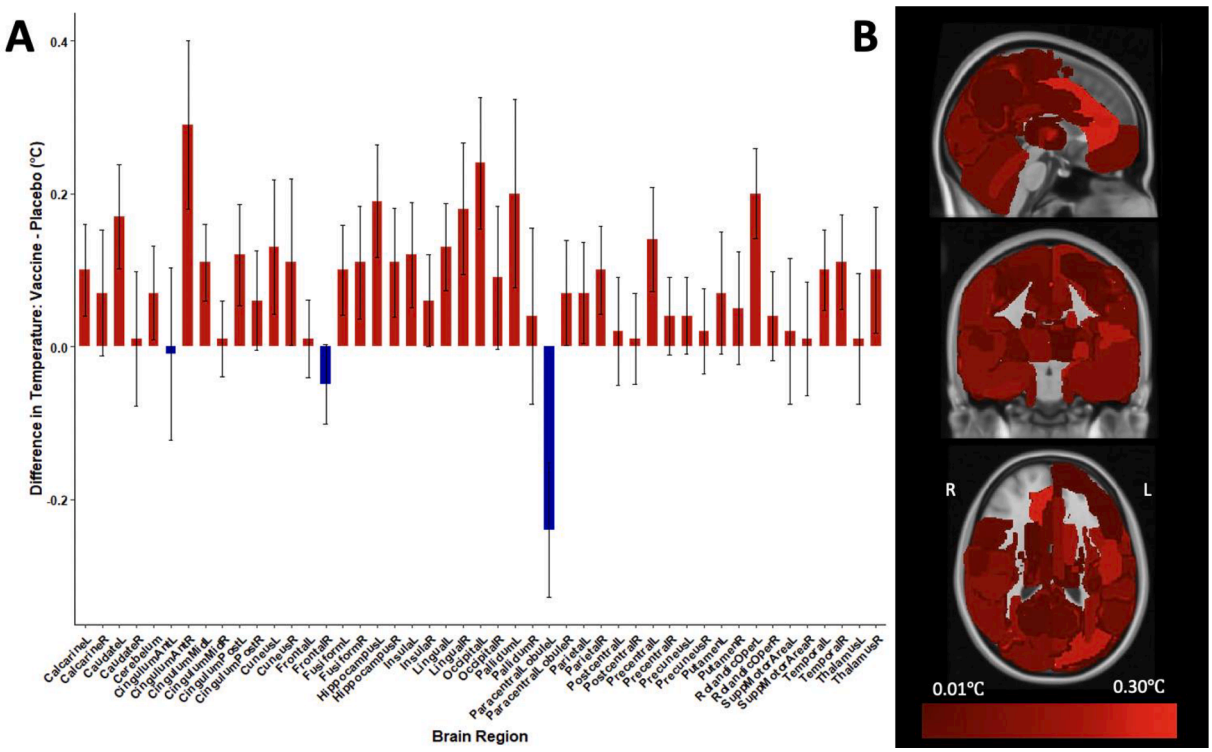

Fig. 3. Mean difference in temperature (post-vaccine – post-placebo) across forty-seven brain regions (A) and colour map of brain regions higher in temperature post-vaccine than post-placebo superimposed on T1-weighted image (B). *Note:* A) Error bars represent standard error. B) 44 regions hand-drawn on T1-weighted MNI standard image using FSL. Temperature increases post-vaccine are represented on a color scale extending from dark red (0.01 °C) to bright red (0.30 °C). The smallest average temperature increase is 0.01 °C in the left mid cingulum and the largest average temperature increase is 0.29 °C in the right anterior cingulum. The three regions that did not increase in temperature post-vaccine (right frontal lobe, left anterior cingulum, and left paracentral lobule) are shown in grey.

Table 2
Brain regions with significant effect of treatment observed on metabolite ratios.

ROI	Metabolite ratio	Vaccine	Placebo	Difference (95% CI) vaccine-placebo	*p*
Paracentral lobule R	MI/CR	0.293 ± 0.020	0.343 ± 0.018	−0.050 (-0.097, −0.004)	0.037
Temporal R	MI/CR	0.486 ± 0.018	0.508 ± 0.017	−0.022 (-0.002, −0.041)	0.031
Calcarine L	MI/CR	0.511 ± 0.011	0.547 ± 0.010	−0.037 (-0.009, −0.064)	0.013
Lingual L	MI/CR	0.462 ± 0.032	0.489 ± 0.032	−0.027 (-0.011, −0.043).	0.003
Caudate R	CHO/CR	0.247 ± 0.006	0.263 ± 0.006	−0.016 (-0.000, −0.031)	0.047
Frontal L	CHO/CR	0.214 ± 0.005	0.209 ± 0.005	0.005 (0.000, 0.010).	0.042

ROI = region of interest; L = left; R = right.

There were several significant correlations between metabolite ratios and mood scores. The most significant post-vaccine mood associations ($p < 0.01$) were with CHO/CR in the left posterior cingulum and NAA/CR in the right hippocampus, right anterior cingulum, cerebellum, and right and left thalamus, as shown in Supplementary Fig. 4. The most significant post-placebo mood associations ($p < 0.001$) were with NAA/CR in the left hippocampus, left middle cingulum, and left parietal lobe and MI/CR in the right and left precuneus, as shown in Supplementary Fig. 5. Correlations between metabolite ratios and mood at 3 h are detailed in Supplementary Tables 10–12.

Table 3
Correlations between body temperature and whole brain temperature at baseline and 3–4 h post-treatment.

		Timepoint			
		Baseline	**0 h**	**3 h**	**4 h**
Treatment	**Placebo**	0.574, 0.008*	0.355, 0.124	0.550, 0.015*	0.638, 0.003*
	Vaccine	0.555, 0.026*	0.539, 0.031*	0.436, 0.070	0.344, 0.162

Data are presented as Spearman rank correlation coefficient, *p* value. Baseline and 0 h timepoints: whole brain temperature assessed at baseline correlated with body temperature at baseline (pre-scan) and 0 h (post-scan, immediately after treatment administration). 3 h and 4 h timepoints: whole brain temperature assessed post-treatment (3–4 h) correlated with body temperature at 3 h (pre-scan) and at 4 h (post-scan).

4. Discussion

4.1. Brain temperature

The present study is the first to investigate the effect of an acute inflammatory stimulus on brain temperature and metabolite ratios in healthy volunteers. More than 90% of 47 brain regions investigated showed an elevation in temperature post-vaccine compared to post-placebo; whole brain temperature, however, did not increase. It is unsurprising that analysis of whole brain temperature did not find an increased temperature post-vaccine given that 1) the regional increases in temperature were very small, and 2) three brain regions decreased in temperature post-vaccine including the right frontal lobe, which is a relatively large region contributing a substantial number of voxels to the

whole brain analysis.

Whole brain temperature elevations have been observed in conditions of high-level inflammation, such as following acute ischaemic stroke (Karaszewski et al., 2009). In conditions of low-level inflammation such as chronic fatigue/myalgic encephalomyelitis, whole brain temperature elevation was not observed; only regional brain temperature elevations were significant (Mueller et al., 2020a). Typhoid vaccine is a mild acute inflammatory stimulus, a more potent inflammatory stimulus such as lipopolysaccharide (LPS) might elicit a greater whole brain temperature difference (Bahador and Cross, 2016) than observed in the present study. It is important to note also that shim imperfections in the frontal and temporal regions compromise the whole brain temperature measurement, perhaps resulting in underestimation. Undersampling occurred (as shown in Supplementary Figs. 1 and 2) particularly in the frontal lobe where a drop in temperature post-vaccine was observed in the right hemisphere. A quality shim is vital for accurate whole brain temperature computation, as discussed further below.

The regions of increased temperature post-vaccine included a variety of both cortical and subcortical regions. The increased temperature in a large number of regions is suggestive of an inflammatory response occurring widely across the brain in response to the vaccine. In a small sample of non-human primates given LPS, an increase in activated microglia was observed in nine brain regions using positron emission tomography (PET) scans one and four hours after administration (Hannestad et al., 2012). The activated microglia were observed in a variety of regions across the brain including the frontal lobe, pallidum, putamen, caudate, brainstem, and insula (Hannestad et al., 2012). Although we did not use LPS in our study, typhoid vaccine produces a similar (though more mild) immune response (Schedlowski et al., 2014). It appears that, like LPS, typhoid vaccine results in widespread inflammatory activity across the brain rather than only in one specific region.

The left occipital lobe and right anterior cingulum showed the greatest increases in brain temperature post-vaccine compared to post-placebo, suggesting heightened microglial activation in these regions. Elevated microglial activation has been observed in the occipital lobe in neuroinflammatory conditions such as traumatic brain injury (Tzourio-Mazoyer et al., 2002) and HIV (Senn, 2002) and in the anterior cingulate in major depressive disorder (Benjamini and Yekutieli, 2001; Bahador and Cross, 2016; Hannestad et al., 2012). The previous experimental study using PET found increased microglial expression in the occipital cortex and cingulate of non-human primates 4 h after endotoxin administration (Schedlowski et al., 2014). In human volunteers, altered glucose metabolism has been observed in the right anterior cingulate following injection of endotoxin (Hannestad et al., 2012); inflammatory cytokines are thought to be involved in impaired brain glucose uptake (Harrison et al., 2009). Our results and prior research strongly indicate a role of the right anterior cingulum and occipital lobe in neuroinflammation; however, reasons for the exacerbated inflammatory response in these regions are unknown. Elevated inflammation in the cingulate, a region linked to both emotional and cognitive processing, may serve to elicit protective 'sickness behaviour', although this becomes a maladaptive mechanism in MDD (Harrison et al., 2009).

Only three regions were not at higher temperature post-vaccine compared to post-placebo. The right frontal lobe, left anterior cingulum, and left paracentral lobule were lower in temperature, although not significantly. It seems unlikely that these regions are exempt from inflammatory activity, given the previous reports that indicate neuroinflammation in these regions (Mueller et al., 2020a; Qiu et al., 2014).

Regions at the edge of the brain, such as the paracentral lobule and frontal lobe, are subject to greater variability than inner regions of the brain (Maudsley et al., 2017). The temperature mapped images in the supplementary material show that the frontal lobes were undersampled relative to the inner regions due to the strict voxel exclusion criteria. A previous report indicated that the brain edges are susceptible to lipid contamination, spatial normalization errors, and increased line-broadening (Maudsley et al., 2017). The frontal lobe is particularly susceptible to missing voxels also because of the 3D rectangular saturation band placed to cover the eyes of each participant (Sharma et al., 2020). The band is a fixed structure and unable to be curved to match the particular structural anatomy of the participant's brain, so the band may 'cut off' a portion of the frontal lobe in some cases.

The anterior cingulum is located near the sinuses; this positioning creates an air-tissue interface, so a good shim is vital to avoid signal dropout due to an inhomogeneous B0 magnetic field. A consensus report used a 3D EPSI sequence to demonstrate that signal dropout may occur in the anterior cingulum if the shimming is inadequate (Wilson et al., 2019). Although the 3D EPSI sequence enables relatively fast MRSI of the whole-brain, a homogeneous B0 field is extremely difficult to obtain across all brain regions at the same time with only second-order shim coils (Wilson et al., 2019). The present study used first- and second-order coils, but recent recommendations suggest higher-order (3 or above) are needed to attain a homogeneous B0 particularly at a 3T field strength and above (Stockmann and Wald, 2018). The average percentage of voxels accepted in the left anterior cingulum was 46%; an improved shim may be needed to avoid signal dropout and therefore capture a larger percentage of voxels in this region.

Higher temperature in the left hemisphere than the right was noted in the paracentral lobule, postcentral lobule, calcarine, caudate, putamen, and frontal lobe. A slightly higher temperature in the left hemisphere relative to the right, as well as a difference in frontal lobe temperature between hemispheres, has been previously noted (Maudsley et al., 2017). Variations in regional and hemispheric temperature is not unusual and has been observed in a number of previous MRSI studies (Maudsley et al., 2017; Zhang et al., 2020). It is unclear whether hemispheric temperature asymmetries are due to physiological differences, or magnetic susceptibility-induced frequency shifts.

4.2. Metabolite ratios

CHO/CR is used in MRSI studies of neuroinflammation as a marker for glial density; considerably higher concentrations of CHO are found in glial cells compared to neurons (Chang et al., 2013). The CHO peak reflects the concentration of water-soluble CHO-containing compounds, including phosphochloline and glycerophosphochloline (Miller et al., 1996). CHO is involved in cellular turnover and cell membrane metabolism (Michaelis et al., 1993) and increased CHO is thought to reflect membrane degradation, oedema, or energy failure (Chang et al., 2013; Quarantelli, 2015). The observed increase in CHO/CR in the left frontal lobe post-vaccine is consistent with prior studies of neuroinflammatory conditions; increased CHO has also been reported in multiple sclerosis (Tartaglia et al., 2002), hepatitis C (Forton et al., 2001), and HIV infection (Lentz et al., 2011). Both increased and decreased CHO/CR have been observed in the frontal lobe of patients with depression (Riley and Renshaw, 2018).

Reduced CHO/CR, observed in the present study in the right caudate, may represent decreased membrane turnover, abnormalities in the function and structure of glial cells and myelination (Glitz et al., 2002; Moore and Bulletin, 2002; Zhang et al., 2015). Decreased CHO has been observed in the right caudate head of patients with bipolar disorder (Port et al., 2008). The literature on CHO/CR in psychiatric disorders, particularly in MDD, are inconsistent, with some studies reporting increases and others decreases in CHO/CR. Nevertheless, the observed alterations in CHO/CR are suggestive of an effect of the inflammatory stimulus at the cellular level, although the precise mechanism remains unknown.

NAA is an abundant amino acid located in the cytoplasm of neurons following its production in the mitochondria from L-aspartate and acetyl-coenzyme-A (Homer, 1967). NAA is involved in a variety of processes including protein synthesis, osmotic regulation and ATP metabolism (Homer, 1967; Birken and Oldendorf, 1989). Decreased NAA is thought to reflect neuronal or axonal damage and has been

observed in bipolar disorder (Winsberg et al., 2000), multiple sclerosis (Caramanos et al., 2005) and Alzheimer's disease (Adalsteinsson et al., 2000). A recent diffusion weighted MRS study found no change in NAA levels in their chosen ROI (the thalamus) following administration of LPS (De Marco et al., 2022), consistent with ex vivo studies that show no effect of LPS on NAA (Chang et al., 2005). Since the typhoid vaccine activates a very similar transient immune response, it is not surprising that we did not observe any change in NAA/CR in our study. The lack of NAA/CR alteration post-vaccine suggests that, like LPS, typhoid vaccine does not affect neuronal morphology. The absence of a treatment effect on NAA/CR is consistent with studies of MDD, where normal neuronal cell numbers were observed and there was no significant alteration in NAA (Yildiz-Yesiloglu and Ankerst, 2006). The metabolite alterations in CHO/CR and MI/CR, and absence of a change in NAA/CR, suggests that typhoid vaccine may elicit a similar inflammatory response to that observed in MDD.

MI is considered a marker of glial content as it is found primarily within astrocytes (Brand et al., 1993). MI is an osmolyte that maintains the integrity of glial cells. MI is also involved in the metabolism of membrane-bound phospholipids and acts as a precursor for secondary messengers to various neuronal signalling systems (Pouwels and Frahm, 1998). An increase in MI/CR may occur due to astrocytosis, gliosis, or breakdown of myelin. Conversely a decrease in MI/CR, as observed in several regions in the present study, could occur due to glial cell loss. Reduced MI/CR has been reported in MDD; the authors noted that the mechanism behind the decrease is ambiguous, but likely reflects glial cell dysfunction or loss (Coupland et al., 2005). Research on MI/CR in psychiatric disorders such as MDD and bipolar disorder is highly variable, both increases and decreases in MI/CR in the frontal regions have been observed and these studies are often underpowered (Yildiz-Yesiloglu and Ankerst, 2006). In alternative low-level neuroinflammatory conditions such as rheumatoid arthritis and ME/CFS, alterations to MI/CR were non-existent or very minimal (Mueller et al., 2020a, Mueller et al., 2020b). Further investigations with larger sample sizes are needed to validate findings suggestive of MI/CR alterations in low-level neuroinflammatory conditions.

4.3. Body temperature

The absence of post-vaccine body temperature changes and lack of association with brain temperature confirmed that brain temperature was not elevated because of an increase in body temperature. Our results are consistent with prior research in which body temperature was not increased following administration of the typhoid vaccine, despite an inflammatory response occurring throughout the body as shown by elevated peripheral inflammatory markers (Strike et al., 2004; Harrison et al., 2015; Wright et al., 2005). Furthermore, a dissociation between brain and body temperature has been noted when injury or trauma occurs to the brain, whereas temperature in the healthy brain tends to correlate with body temperature (Karaszewski et al., 2013; Childs et al., 2007). The absence of association between body temperature and whole brain temperature after the vaccine may indicate that neuroinflammation has occurred, particularly since brain and body temperature were correlated at other timepoints including post-placebo.

4.4. Mood

We did not observe a significant drop in mood following administration of the vaccine. Prior work noted a small but significant decrease in mood between two and four hours post-vaccine that was not present post-placebo (Strike et al., 2004; Maudsley et al., 2009; Harrison et al., 2009). In the present study, the overall mood trajectories following placebo and vaccine were similar; although of note is that mood increased at 2 h following placebo but decreased at 2 h following the vaccine (Fig. 4). The difference was too small to reach significance, however the trend is towards that shown in previous work. The methods

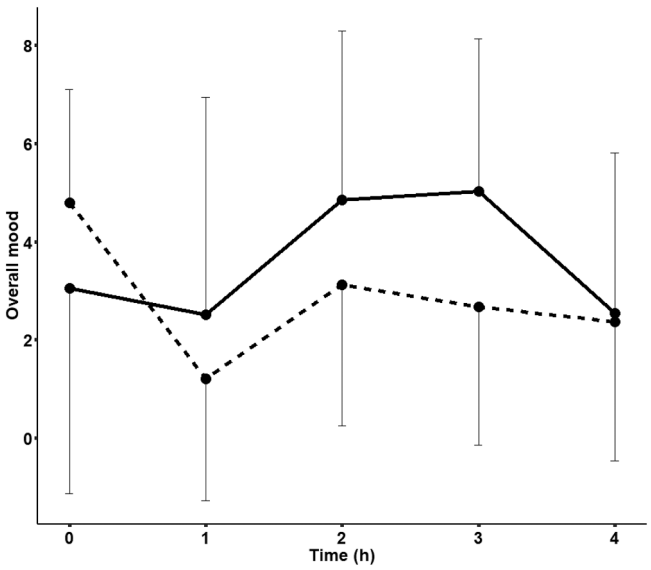

Fig. 4. Trajectory of overall mood (mean ± SEM) following vaccine (dashed line) and placebo (solid line) administration.

in our study are very similar to previous investigations, so the absence of any significant effect of treatment on mood was unexpected. A possible reason is that the characteristics of our sample may have differed from those in prior studies. Previous studies showed that the inflammatory response of the typhoid vaccine was modulated by stress and loneliness, and that financial strain was associated with worse mood following the vaccine (Brydon et al., 2009a, Brydon et al., 2009b). We did not specifically investigate these factors; however, the baseline POMS scores suggest that our sample is similar to those in prior studies so this possibility seems unlikely. The observed decrease in mood in the earlier studies was modest, and other factors we had not considered may have influenced the mood responses in our study.

The number of significant associations between regional brain temperatures and mood subscales was considerably higher post-vaccine compared to post-placebo at both the 3 h and 4 h time points. These results indicated a relationship between neuroinflammation and mood, though we are unable to determine any cause and effect. The most likely hypothesis is that the inflammatory activity leads to increased regional brain temperature, which then results in associated negative mood changes. This hypothesis would also account for the mood changes observed in inflammatory mood disorders such as MDD. Prior research hypothesises a link between brain temperature and mood disorders, such that therapeutic modification of brain temperature may be a key factor involved in the resolution of mood disturbances (Crespi, 2018; Salerian et al., 2008).

We cannot determine from the present study whether brain temperature is linked directly to mood, or if there is another factor involved in the neuroinflammation that causes the observed associations. Metabolite alterations are likely involved in the relationship between brain temperature and mood, as indicated by the associations observed in the present study. It is of note, however, that we observed a much larger number of associations between brain temperature and mood than between metabolite ratios and mood indicating that inflammation-related brain temperatures are associated with mood, even without alterations to the metabolite ratios. Microglial activation, hypothesised to cause elevated brain temperature, does not always co-occur with metabolite alterations; the inflammatory processes are somewhat distinct. Metabolite alterations are therefore unlikely to be a key factor causing the associations between brain temperature and mood.

We observed several correlations between regional metabolite alterations and mood scores both post-vaccine and post-placebo. Different brain regions were involved post-vaccine versus post-placebo,

suggesting that different brain regions are involved in mood regulation during neuroinflammation compared to the healthy brain. In the healthy brain, we found new evidence that metabolite alterations in the left mid cingulum, left parietal lobe, left hippocampus, and precuneus were linked to mood. It is important to note, however, that at least two-thirds of the post-placebo correlations appeared to be driven largely by outliers (see Supplementary Fig. 5), whereas the post-vaccine correlations appeared more evenly distributed and robust. In the inflamed brain, alterations in CHO/CR in the left posterior cingulum and NAA/CR in the right hippocampus, right anterior cingulum, cerebellum, and right and left thalamus appeared to impact mood. These findings are supported by studies of mood disorders; alterations of CHO/CR and NAA/CR in the same regions have been implicated to varying levels in bipolar disorder (Li et al., 2016; Lai et al., 2019) and schizophrenia (Ende et al., 2003). Reduced symptomatology of mood disorders has been observed alongside post-treatment alterations of NAA/CR and CHO/CR (Soeiro-de-Souza et al., 2021; Gonul et al., 2006); the anti-inflammatory effects of treatment on NAA/CR and CHO/CR may assist in improving mood, particularly if these metabolite alterations occur in regions with emotion regulation functions. Further MRSI investigations on patients with mood disorders are needed to better understand the links between metabolite ratios, neuroinflammation, and mood.

5. Strengths and limitations

The primary strength of this study is the novelty of the investigation; we examined for the first time the impact of an acute inflammatory stimulus on brain temperature and metabolite ratios, as well as links between mood and brain temperature, in healthy volunteers. An additional strength of the study is the use of state-of-the-art magnetic resonance spectroscopy for measurement of brain temperature. While the sample size is small given that this study is essentially a proof-of-concept, the use of a crossover design with each participant acting as their own control allows fewer participants than would be required for a parallel groups design to achieve the same statistical power. Blinding of the participants and investigators to the treatment allocations is also a strength. Double-blinding was used to avoid biased mood assessments as well as potential neurobiological effects which may have impacted the brain temperature and metabolite ratios; both self-report and more supposedly objective measures such as brain scans may be impacted by participant and/or investigator expectations (Ropper et al., 2020).

Spatial inhomogeneities are a critical limitation of all MRSI data so a good shim is essential. First and second order shim coils were used as recommended in conjunction with an interactive shimming procedure; however, undersampling remains an issue particularly in the frontal-temporal regions where spectra may be contaminated by lipids. 3D EPSI was used because of the good consistency and high-quality spectra evident from previous studies, in addition to the fast and clinically viable scan times. However, magnetic inhomogeneity is a problem in whole brain MRSI as it is virtually impossible to achieve a homogenous magnetic field across the whole brain simultaneously. Strict quality criteria were implemented during processing to minimise the impact of inhomogeneities on the data.

Frequency drift from instrumentation factors, such as heating of the gradient coil, or patient motion may have impacted the data obtained. However, the metabolite and water reference data should be equally affected due to the interleaved sequence used for acquisition. Furthermore, a frequency drift correction was applied during data processing which has been shown to improve accuracy (Ebel and Maudsley, 2005). Frequency shifts due to magnetic susceptibility and those due to spatial variations in temperature cannot be separated, so it is important to emphasise that temperatures are estimations rather than exact. Additionally, the water and metabolite datasets were collected using different TE lengths, resulting in eddy currents that cannot be fully compensated and therefore may compromise the accuracy of the temperature estimates. Although this aspect creates a source of bias, it is not intervention-dependent so is of limited importance. Furthermore, prior MRSI-derived brain temperatures demonstrate good reliability across studies and correlate well with measurements from phantoms (Thrippleton et al., 2014).

Metabolites were quantified as ratios to enable comparison with other similar studies; however, it has been suggested that total metabolite quantification may be a more reliable measure (Jansen et al., 2006). Furthermore, CR was used as the reference metabolite due to its stability across grey and white matter, and uniform distribution. However, some evidence suggests using CR ratios can be misleading (Li et al., 2003). Variation in creatine concentrations have been observed in mood disorders such as schizophrenia (Öngür et al., 2009), so an alternative reference metabolite or total metabolite quantification may be a preferable option for future studies using MRSI on clinical populations.

Finally, there are a number of other factors that may have impacted the brain temperature observed in the present study. Time of day, physical activity, and hormonal fluctuations may have influenced the brain temperature estimates. The crossover design provided benefit in this regard with participants acting as their own controls. However, considering the clinical viability of brain temperature as a screening or diagnostic tool there is undoubted merit in data which are based on sample characteristics which are not unrealistically homogeneous. Such data are essential to fully understand the reliability and potential application of MRSI temperature estimations.

6. Conclusion

The present study is the first investigation of the effect of an acute inflammatory stimulus on brain temperature and metabolite ratios in healthy volunteers. The results show a mild inflammatory effect in the brain, as indicated by alterations to regional brain temperature. The greater proportion of brain regions at a higher temperature post-vaccine compared to placebo indicates a small but noticeable effect of inflammation on brain temperature. The findings of this study may apply to measurement of low-level neuroinflammation in individuals with psychiatric disorders such as MDD. Few studies have so far been conducted using the novel MRSI/EPSI techniques utilised in the present study. Further research using these techniques will provide greater understanding of the pathophysiology and consequences of neuroinflammation.

Funding

This work was supported by the Maurice & Phyllis Paykel Trust, New Zealand Pharmacy Education and Research Foundation, and the Oakley Mental Health Research Foundation. JCL was the recipient of a Neurological Foundation Repatriation Fellowship.

Ethical approval

All procedures performed in studies involving human participants were in accordance with the ethical standards of the institutional and/or national research committee and with the 1964 Helsinki declaration and its later amendments or comparable ethical standards.

Informed consent

Informed consent was obtained from all individual participants included in the study.

CRediT authorship contribution statement

Julia R. Plank: Investigation, Formal analysis, Writing – original draft, Visualization. **Catherine Morgan:** Methodology, Software, Writing – review & editing. **Frederick Sundram:** Resources. **Lindsay D. Plank:** Formal analysis, Writing – review & editing. **Nicholas Hoeh:**

Resources. **Sinyeob Ahn:** Software. **Suresh Muthukumaraswamy:** Methodology, Resources. **Joanne C. Lin:** Methodology, Funding acquisition, Supervision.

Declaration of Competing Interest

The authors declare that they have no known competing financial interests or personal relationships that could have appeared to influence the work reported in this paper.

Acknowledgements

We sincerely thank all participants in this research. We also extend our gratitude to Sarah McGrannachan, Dr Rachael Sumner, Joseph Chen, Dr Anne Horne, Keryl Cunningham, Sulaiman Sheriff, and the staff at the Centre for Advanced MRI for their assistance with the study.

Appendix A. Supplementary data

Supplementary data to this article can be found online at https://doi.org/10.1016/j.nicl.2022.103053.

References

Ackerman, J., Gadian, D., Radda, G., et al., 1969. Observation of 1H NMR signals with receiver coils tuned for other nuclides. J. Magn. Reson. 42 (3), 498–500.
Adalsteinsson, E., Sullivan, E.V., Kleinhans, N., Spielman, D.M., Pfefferbaum, A., 2000. Longitudinal decline of the neuronal marker N-acetyl aspartate in Alzheimer's disease. Lancet 355 (9216), 1696–1697.
Babourina-Brooks, B., Wilson, M., Arvanitis, T.N., Peet, A.C., Davies, N.P., 2014. MRS water resonance frequency in childhood brain tumours: A novel potential biomarker of temperature and tumour environment. NMR Biomed. 27 (10), 1222–1229. https://doi.org/10.1002/nbm.3177.
Bahador, M., Cross, A.S., 2016. From therapy to experimental model: a hundred years of endotoxin administration to human subjects. J. Endotoxin Res. 13 (5), 251–279. https://doi.org/10.1177/0968051907085986.
Benjamini, Y., Yekutieli, D., 2001. The control of the false discovery rate in multiple testing under dependency. Ann. Stat. 1165–1188.
Birken, D.L., Oldendorf, W.H., 1989. N-Acetyl-L-Aspartic acid: A literature review of a compound prominent in 1H-NMR spectroscopic studies of brain. Neurosci. Biobehav. Rev. 13 (1), 23–31. https://doi.org/10.1016/S0149-7634(89)80048-X.
Brand, A., Richter-Landsberg, C., Leibfritz, D., 1993. Multinuclear NMR studies on the energy metabolism of glial and neuronal cells. Dev. Neurosci. 15 (3–5), 289–298. https://doi.org/10.1159/000111347.
Brydon, L., Walker, C., Wawrzyniak, A.J., Chart, H., Steptoe, A., 2009a. Dispositional optimism and stress-induced changes in immunity and negative mood. Brain Behav. Immun. 23 (6), 810–816. https://doi.org/10.1016/J.BBI.2009.02.018.
Brydon, L., Walker, C., Wawrzyniak, A., Whitehead, D., Okamura, H., Yajima, J., Tsuda, A., Steptoe, A., 2009b. Synergistic effects of psychological and immune stressors on inflammatory cytokine and sickness responses in humans. Brain Behav. Immun. 23 (2), 217–224.
Cady, E.B., D'Souza, P.C., Penrice, J., Lorek, A., 1995. The estimation of local brain temperature by in vivo 1H magnetic resonance spectroscopy. Magn. Reson. Med. 33 (6), 862–867. https://doi.org/10.1002/mrm.1910330620.
Caramanos, Z., Narayanan, S., Arnold, D.L., 2005. 1H-MRS quantification of tNA and tCr in patients with multiple sclerosis: A meta-analytic review. Brain. 128 (11), 2483–2506. https://doi.org/10.1093/brain/awh640.
Chang, S.L., Cloak, C.C., Malellari, L., Chang, L., 2005. The effects of repeated endotoxin exposure on rat brain metabolites as measured by ex vivo 1HMRS. J. Neuroimmunol. 166 (1–2), 39–46. https://doi.org/10.1016/J.JNEUROIM.2005.04.021.
Chang, L., Munsaka, S.M., Kraft-Terry, S., Ernst, T., 2013. Magnetic resonance spectroscopy to assess neuroinflammation and neuropathic pain. J. Neuroimmune Pharmacol. 8 (3), 576–593. https://doi.org/10.1007/s11481-013-9460-x.
Chen, J., Buchanan, J.B., Sparkman, N.L., Godbout, J.P., Freund, G.G., Johnson, R.W., 2008. Neuroinflammation and disruption in working memory in aged mice after acute stimulation of the peripheral innate immune system. Brain Behav. Immun. 22 (3), 301–311. https://doi.org/10.1016/J.BBI.2007.08.014.
Childs, C., Hiltunen, Y., Vidyasagar, R., Kauppinen, R.A., 2007. Determination of regional brain temperature using proton magnetic resonance spectroscopy to assess brain–body temperature differences in healthy human subjects. Magn. Reson. Med. 57 (1), 59–66.
Clark, J.B., 1998. N-acetyl aspartate: a marker for neuronal loss or mitochondrial dysfunction. Dev. Neurosci. 20 (4–5), 271–276.
Coupland, N.J., Ogilvie, C.J., Hegadoren, K.M., Seres, P., Hanstock, C.C., Allen, P.S., 2005. Decreased prefrontal myo-inositol in major depressive disorder. Biol. Psychiatry 57 (12), 1526–1534. https://doi.org/10.1016/J.BIOPSYCH.2005.02.027.
Crespi, F., 2018. Brain temperature and brain metabolism measurements: rapid in vivo markers of mood i.e. mania or depressive disorders. Biol. Eng. Med. 3 (4), 1–2. https://doi.org/10.15761/BEM.1000148.
De Marco, R., Ronen, I., Branzoli, F., Amato, M.L., Asllani, I., Colasanti, A., Harrison, N. A., Cercignani, M., 2022. Diffusion-weighted MR spectroscopy (DW-MRS) is sensitive to LPS-induced changes in human glial morphometry: a preliminary study. Brain Behav. Immun. 99, 256–265.
Ebel, A., Maudsley, A.A., 2003. Improved spectral quality for 3D MR spectroscopic imaging using a high spatial resolution acquisition strategy. Magn. Reson. Imaging 21 (2), 113–120. https://doi.org/10.1016/S0730-725X(02)00645-8.
Ebel, A., Maudsley, A.A., 2005. Detection and correction of frequency instabilities for volumetric 1H echo-planar spectroscopic imaging. Magn. Reson. Med. 53 (2), 465–469. https://doi.org/10.1002/MRM.20367.
Ende, G., Braus, D.F., Walter, S., Weber-Fahr, W., Henn, F.A., 2003. Multiregional 1H-MRSI of the hippocampus, thalamus, and basal ganglia in schizophrenia. Eur. Arch. Psychiatry Clin. Neurosci. 253 (1), 9–15.
Forton, D.M., Allsop, J.M., Main, J., Foster, G.R., Thomas, H.C., Taylor-Robinson, S.D., 2001. Evidence for a cerebral effect of the hepatitis C virus. Lancet 358 (9275), 38–39. https://doi.org/10.1016/S0140-6736(00)05270-3.
Glitz, D., Manji, H., Moore, G.J., 2002. Mood disorders: treatment-induced changes in brain neurochemistry and structure. Seminars in Clinical Neuropsychiatry. 7 (4), 269–280. https://doi.org/10.1053/scnp.2002.35226.
Godbout, J.P., Chen, J., Abraham, J., Richwine, A.F., Berg, B.M., Kelley, K.W., Johnson, R.W., 2005. Exaggerated neuroinflammation and sickness behavior in aged mice after activation of the peripheral innate immune system. FASEB J. 19 (10), 1329–1331.
Goldsmith, D.R., Rapaport, M.H., Miller, B.J., 2016. A meta-analysis of blood cytokine network alterations in psychiatric patients: comparisons between schizophrenia, bipolar disorder and depression. Mol. Psychiatry 21 (12), 1696–1709. https://doi.org/10.1038/MP.2016.3.
Gonul, A.S., Kitis, O., Ozan, E., Akdeniz, F., Eker, C., Eker, O.D., Vahip, S., 2006. The effect of antidepressant treatment on N-acetyl aspartate levels of medial frontal cortex in drug-free depressed patients. Prog. Neuro-Psychopharmacol. Biol. Psychiatry 30 (1), 120–125.
Govindaraju, V., Young, K., Maudsley, A.A., 2000. Proton NMR chemical shifts and coupling constants for brain metabolites. NMR Biomed. 13 (3), 129–153. https://doi.org/10.1002/1099-1492.
Hannestad, J., Subramanyam, K., DellaGioia, N., Planeta-Wilson, B., Weinzimmer, D., Pittman, B., Carson, R.E., 2012. Glucose metabolism in the insula and cingulate is affected by systemic inflammation in humans. J. Nucl. Med. 53 (4), 601–607.
Hannestad, J., Gallezot, J.-D., Schafbauer, T., Lim, K., Kloczynski, T., Morris, E.D., Carson, R.E., Ding, Y.-S., Cosgrove, K.P., 2012. Endotoxin-induced systemic inflammation activates microglia: [11C]PBR28 positron emission tomography in nonhuman primates. Neuroimage. 63 (1), 232–239.
Harrison, N.A., Brydon, L., Walker, C., Gray, M.A., Steptoe, A., Dolan, R.J., Critchley, H. D., 2009. Neural origins of human sickness in interoceptive responses to inflammation. Biol. Psychiatry 66 (5), 415–422.
Harrison, N.A., Brydon, L., Walker, C., Gray, M.A., Steptoe, A., Critchley, H.D., 2009. Inflammation causes mood changes through alterations in subgenual cingulate activity and mesolimbic connectivity. *Biol. Psychiatry* 66 (5), 407–414.
Harrison, N.A., Cooper, E., Dowell, N.G., Keramida, G., Voon, V., Critchley, H.D., Cercignani, M., 2015. Quantitative magnetization transfer imaging as a biomarker for effects of systemic inflammation on the brain. Biol. Psychiatry 78 (1), 49–57.
Hindman, J.C., 1966. Proton resonance shift of water in the gas and liquid states. J. Chem. Phys. 44 (12), 4582–4592. https://doi.org/10.1063/1.1726676.
Homer, K., 1967. The enzymatic synthesis of N-acetyl-L-aspartic acid by a water-insoluble preparation of a cat brain acetone powder. J. Biol. Chem. 242 (20), 4619–4622.
Jansen, J.F.A., Backes, W.H., Nicolay, K., Kooi, M.E., 2006. 1H MR spectroscopy of the brain: absolute quantification of metabolites. Radiology 240 (2), 318–332. https://doi.org/10.1148/RADIOL.2402050314.
Kanai, Y., Nakamura, M., Kikuma, N., Yasui, G.O., Takada, K., 2001. Effect of temperature and pH on the chemical shift of metabolites in proton-MRS. Japanese J. Radiol. Technol. 57 (6), 651–656.
Karaszewski, B., Wardlaw, J.M., Marshall, I., Cvoro, V., Wartolowska, K., Haga, K., Armitage, P.A., Bastin, M.E., Dennis, M.S., 2009. Early brain temperature elevation and anaerobic metabolism in human acute ischaemic stroke. Brain 132 (4), 955–964.
Karaszewski, B., Carpenter, T.K., Thomas, R.GR., Armitage, P.A., Lymer, G.K.S., Marshall, I., Dennis, M.S., Wardlaw, J.M., 2013. Relationships between brain and body temperature, clinical and imaging outcomes after ischemic stroke. J. Cereb. Blood Flow Metab. 33 (7), 1083–1089.
Kirov, I.I., Patil, V., Babb, J.S., Rusinek, H., Herbert, J., Gonen, O., 2009. MR spectroscopy indicates diffuse multiple sclerosis activity during remission. J. Neurol. Neurosurg. Psychiatry 80 (12), 1330–1336.
Lai, S., Zhong, S., Shan, Y., Wang, Y., Chen, G., Luo, X., Chen, F., Zhang, Y., Shen, S., Huang, H., Ning, Y., Jia, Y., 2019. Altered biochemical metabolism and its lateralization in the cortico-striato-cerebellar circuit of unmedicated bipolar II depression. J. Affect. Disord. 259, 82–90.
Lentz, M.R., Kim, W.K., Kim, H., et al., 2011. Alterations in brain metabolism during the first year of HIV infection. J. NeuroVirol. 17 (3), 220–229. https://doi.org/10.1007/S13365-011-0030-9/TABLES/4.
Li, B., Wang, H., Gonen, O., 2003. Metabolite ratios to assumed stable creatine level may confound the quantification of proton brain MR spectroscopy. Magn. Reson. Imaging 21 (8), 923–928. https://doi.org/10.1016/S0730-725X(03)00181-4.
Li, H., Xu, H., Zhang, Y., Guan, J., Zhang, J., Xu, C., Shen, Z., Xiao, B.o., Liang, C., Chen, K., Zhang, J., Wu, R., 2016. Differential neurometabolite alterations in brains of medication-free individuals with bipolar disorder and those with unipolar depression: a two-dimensional proton magnetic resonance spectroscopy study. Bipolar Disord. 18 (7), 583–590.

Maudsley, A.A., Domenig, C., Govind, V., Darkazanli, A., Studholme, C., Arheart, K., Bloomer, C., 2009. Mapping of brain metabolite distributions by volumetric proton MR spectroscopic imaging (MRSI). Magn. Reson. Med. 61 (3), 548–559.
Maudsley, A.A., Goryawala, M.Z., Sheriff, S., 2017. Effects of tissue susceptibility on brain temperature mapping. Neuroimage. 146, 1093–1101. https://doi.org/10.1016/j.neuroimage.2016.09.062.
McNair, D.M., Lorr, M., Droppleman, L.F., 1971. Manual for the Profile of Mood States. Educational and Industrial Testing Services, San Diego, CA.
Michaelis, T., Merboldt, K.D., Bruhn, H., Hanicke, W., Frahm, J., 1993. Absolute concentrations of metabolites in the adult human brain in vivo: quantification of localized proton MR spectra. Radiology 187 (1), 219–227. https://doi.org/10.1148/radiology.187.1.8451417.
Miller, B.L., Changl, L., Booth, R., Ernst, T., Cornford, M., Nikas, D., McBride, D., Jenden, D.J., 1996. In vivo 1H MRS choline: Correlation with in vitro chemistry/histology. Life Sci. 58 (22), 1929–1935.
Moore, G., Bulletin, M.G.P., 2002. Magnetic resonance spectroscopy: neurochemistry and treatment effects in affective disorders. Psychopharmacol. Bull. 36 (2), 5–23.
Moshkin, M., Akulov, A., Petrovski, D., et al., 2014. Proton magnetic resonance spectroscopy of brain metabolic shifts induced by acute administration of 2-deoxy-d-glucose and lipopolysaccharides. NMR Biomed. 27 (4), 399–405. https://doi.org/10.1002/nbm.3074.
Mueller, C., Lin, J.C., Sheriff, S., Maudsley, A.A., Younger, J.W., 2020a. Evidence of widespread metabolite abnormalities in Myalgic encephalomyelitis/chronic fatigue syndrome: assessment with whole-brain magnetic resonance spectroscopy. Brain Imag. Behav. 14 (2), 562–572. https://doi.org/10.1007/s11682-018-0029-4.
Mueller, C., Lin, J.C., Thannickal, H.H., et al., 2020b. No evidence of abnormal metabolic or inflammatory activity in the brains of patients with rheumatoid arthritis: results from a preliminary study using whole-brain magnetic resonance spectroscopic imaging (MRSI). Clin. Rheumatol. 39 (6), 1765–1774. https://doi.org/10.1007/S10067-019-04923-5/FIGURES/3.
Najjar, S., Pearlman, D.M., Alper, K., Najjar, A., Devinsky, O., 2013. Neuroinflammation and psychiatric illness. J. Neuroinflamm. 10 https://doi.org/10.1186/1742-2094-10-43.
Omori, M., Pearce, J., Komoroski, R.A., Griffin, W.S.T., Mrak, R.E., Husain, M.M., Karson, C.N., 1997. 1997 undefined. In vitro 1H-magnetic resonance spectroscopy of postmortem brains with schizophrenia. Biol. Psychiatry 42 (5), 359–366.
Öngür, D., Prescot, A.P., Jensen, J.E., Cohen, B.M., Renshaw, P.F., 2009. Creatine abnormalities in schizophrenia and bipolar disorder. Psychiatry Res.: Neuroimag. 172 (1), 44–48. https://doi.org/10.1016/J.PSCYCHRESNS.2008.06.002.
Osimo, E.F., Cardinal, R.N., Jones, P.B., Khandaker, G.M., 2018. Prevalence and correlates of low-grade systemic inflammation in adult psychiatric inpatients: An electronic health record-based study. Psychoneuroendocrinology 91, 226. https://doi.org/10.1016/J.PSYNEUEN.2018.02.031.
Ota, M., Sato, N., Sakai, K., Okazaki, M., Maikusa, N., Hattori, K., Hori, H., Teraishi, T., Shimoji, K., Yamada, K., Kunugi, H., 2014. Altered coupling of regional cerebral blood flow and brain temperature in schizophrenia compared with bipolar disorder and healthy subjects. J. Cereb. Blood Flow Metab. 34 (12), 1868–1872.
Port, J.D., Unal, S.S., Mrazek, D.A., Marcus, S.M., 2008. Metabolic alterations in medication-free patients with bipolar disorder: A 3T CSF-corrected magnetic resonance spectroscopic imaging study. Psychiatry Res.: Neuroimaging 162 (2), 113–121. https://doi.org/10.1016/J.PSCYCHRESNS.2007.08.004.
Pouwels, P.J.W., Frahm, J., 1998. Regional metabolite concentrations in human brain as determined by quantitative localized proton MRS. Magn. Reson. Med. 39 (1), 53–60. https://doi.org/10.1002/mrm.1910390110.
Qiu, L., Lui, S., Kuang, W., Huang, X., Li, J., Li, J., Zhang, J., Chen, H., Sweeney, J.A., Gong, Q., 2014. Regional increases of cortical thickness in untreated, first-episode major depressive disorder. Transl. Psychiatry 4 (4), e378–e.
Quarantelli, M., 2015. MRI/MRS in neuroinflammation: methodology and applications. Clin. Transl. Imag. 3 (6), 475–489. https://doi.org/10.1007/s40336-015-0142-y.
Riley, C.A., Renshaw, P.F., 2018. Brain choline in major depression: A review of the literature. Psychiatry Res.: Neuroimag. 271, 142–153. https://doi.org/10.1016/J.PSCYCHRESNS.2017.11.009.
Ropper, A.H., Colloca, L., Barsky, A.J., 2020. Placebo and Nocebo effects. N. Engl. J. Med. 382 (6), 554–561.
Salerian, A.J., Saleri, N.G., Salerian, J.A., 2008. Brain temperature may influence mood: a hypothesis. Med. Hypotheses 70 (3), 497–500. https://doi.org/10.1016/J.MEHY.2007.06.032.
Schain, M., Kreisl, W.C., 2017. Neuroinflammation in neurodegenerative disorders—a review. Curr. Neurol. Neurosci. Rep. 17 (3) https://doi.org/10.1007/s11910-017-0733-2.
Schedlowski, M., Engler, H., Grigoleit, J.S., 2014. Endotoxin-induced experimental systemic inflammation in humans: A model to disentangle immune-to-brain communication. Brain Behav. Immun. 35, 1–8. https://doi.org/10.1016/j.bbi.2013.09.015.
Senn, S., 2002. Cross-over Trials in Clinical Research. John Wiley & Sons.
Sharma, A.A., Nenert, R., Mueller, C., Maudsley, A.A., Younger, J.W., Szaflarski, J.P., 2020. Repeatability and reproducibility of in-vivo brain temperature measurements. Front. Hum. Neurosci. 14, 573. https://doi.org/10.3389/FNHUM.2020.598435/FULL.
Soeiro-de-Souza, M.G., Scotti-Muzzi, E., Fernandes, F., De Sousa, R.T., Leite, C.C., Otaduy, M.C., Machado-Vieira, R., 2021. Anterior cingulate cortex neuro-metabolic changes underlying lithium-induced euthymia in bipolar depression: A longitudinal 1H-MRS study. Eur. Neuropsychopharmacol. 49, 93–100.
Stockmann, J.P., Wald, L.L., 2018. In vivo B0 field shimming methods for MRI at 7 T. NeuroImage. 168, 71–87. https://doi.org/10.1016/J.NEUROIMAGE.2017.06.013.
Strike, P.C., Wardle, J., Steptoe, A., 2004. Mild acute inflammatory stimulation induces transient negative mood. J. Psychosom. Res. 57 (2), 189–194. https://doi.org/10.1016/S0022-3999(03)00569-5.
Sumida, K., Sato, N., Ota, M., Sakai, K., Sone, D., Yokoyama, K., Kimura, Y., Maikusa, N., Imabayashi, E., Matsuda, H., Kunimatsu, A., Ohtomo, K., 2016. Intraventricular temperature measured by diffusion-weighted imaging compared with brain parenchymal temperature measured by MRS in vivo. NMR Biomed. 29 (7), 890–895.
Tartaglia, M.C., Narayanan, S., De Stefano, N., Arnaoutelis, R., Antel, S.B., Francis, S.J., Santos, A.C., Lapierre, Y., Arnold, D.L., 2002. Choline is increased in pre-lesional normal appearing white matter in multiple sclerosis. J. Neurol. 249 (10), 1382–1390.
Thrippleton, M.J., Parikh, J., Harris, B.A., Hammer, S.J., Semple, S.I.K., Andrews, P.J.D., Wardlaw, J.M., Marshall, I., 2014. Reliability of MRSI brain temperature mapping at 1.5 and 3 T. NMR Biomed. 27 (2), 183–190.
Tzourio-Mazoyer, N., Landeau, B., Papathanassiou, D., Crivello, F., Etard, O., Delcroix, N., Mazoyer, B., Joliot, M., 2002. Automated anatomical labeling of activations in SPM using a macroscopic anatomical parcellation of the MNI MRI single-subject brain. Neuroimage. 15 (1), 273–289.
Whiteley, W.N., Thomas, R., Lowe, G., Rumley, A., Karaszewski, B., Armitage, P., Marshall, I., Lymer, K., Dennis, M., Wardlaw, J., 2012. Do acute phase markers explain body temperature and brain temperature after ischemic stroke? Neurology. 79 (2), 152–158.
Wilson, M., Andronesi, O., Barker, P.B., Bartha, R., Bizzi, A., Bolan, P.J., Brindle, K.M., Choi, I.-Y., Cudalbu, C., Dydak, U., Emir, U.E., Gonzalez, R.G., Gruber, S., Gruetter, R., Gupta, R.K., Heerschap, A., Henning, A., Hetherington, H.P., Huppi, P. S., Hurd, R.E., Kantarci, K., Kauppinen, R.A., Klomp, D.W.J., Kreis, R., Kruiskamp, M.J., Leach, M.O., Lin, A.P., Luijten, P.R., Marjańska, M., Maudsley, A. A., Meyerhoff, D.J., Mountford, C.E., Mullins, P.G., Murdoch, J.B., Nelson, S.J., Noeske, R., Öz, G., Pan, J.W., Peet, A.C., Poptani, H., Posse, S., Ratai, E.-M., Salibi, N., Scheenen, T.W.J., Smith, I.C.P., Soher, B.J., Tkáč, I., Vigneron, D.B., Howe, F.A., 2019. Methodological consensus on clinical proton MRS of the brain: Review and recommendations. Magn. Reson. Med. 82 (2), 527–550.
Winsberg, M.E., Sachs, N., Tate, D.L., Adalsteinsson, E., Spielman, D., Ketter, T.A., 2000. Decreased dorsolateral prefrontal N-acetyl aspartate in bipolar disorder. Biol. Psychiatry 47 (6), 475–481.
Wright, C.E., Strike, P.C., Brydon, L., Steptoe, A., 2005. Acute inflammation and negative mood: mediation by cytokine activation. Brain, Behav., Immun. 19 (4), 345–350.
Yildiz-Yesiloglu, A., Ankerst, D.P., 2006. Neurochemical alterations of the brain in bipolar disorder and their implications for pathophysiology: A systematic review of the in vivo proton magnetic resonance spectroscopy findings. Prog. Neuro-Psychopharmacol. Biol. Psychiatry 30 (6), 969–995. https://doi.org/10.1016/J.PNPBP.2006.03.012.
Yildiz-Yesiloglu, A., Ankerst, D.P., 2006. Review of 1H magnetic resonance spectroscopy findings in major depressive disorder: A meta-analysis. Psychiatry Res.: Neuroimaging 147 (1), 1–25. https://doi.org/10.1016/J.PSCYCHRESNS.2005.12.004.
Zhang, Y., Brady, M., Smith, S., 2001. Segmentation of brain MR images through a hidden Markov random field model and the expectation-maximization algorithm. IEEE Trans. Med. Imaging 20 (1), 45–57. https://doi.org/10.1109/42.906424.
Zhang, Y., Han, Y., Wang, Y., et al., 2015. A MRS study of metabolic alterations in the frontal white matter of major depressive disorder patients with the treatment of SSRIs. BMC Psychiatry. 15 (1), 1–7. https://doi.org/10.1186/S12888-015-0489-7/TABLES/3.
Zhang, Y., Taub, E., Mueller, C., Younger, J., Uswatte, G., DeRamus, T.P., Knight, D.C., 2020. Reproducibility of whole-brain temperature mapping and metabolite quantification using proton magnetic resonance spectroscopy. NMR Biomed. 33 (7), e4313. https://doi.org/10.1002/NBM.4313.